

# Cross sections for Coulomb and nuclear breakup of three-body halo nuclei

E. Garrido

*Instituto de Estructura de la Materia, CSIC, Serrano 123, E-28006 Madrid, Spain*

D.V. Fedorov and A.S. Jensen

*Institute of Physics and Astronomy, Aarhus University, DK-8000 Aarhus C, Denmark*

(October 29, 2018)

All possible dissociation cross sections for the loosely bound three-body halo nuclei  ${}^6\text{He}$  ( $n+n+\alpha$ ) and  ${}^{11}\text{Li}$  ( $n+n+{}^9\text{Li}$ ) are computed as functions of target and beam energy. Both Coulomb and nuclear interactions are included in the same theoretical framework. The measurements agree with the calculations for energies above 100 MeV/nucleon. The largest cross sections correspond to final states with zero or three particles for heavy and with two neutrons for light targets.

PACS number(s): 25.60.-t, 25.10.+s, 21.45.+v

*Introduction.* Halo nuclei are spatially extended bound systems [1–4]. Their existence is revealed by large total interaction cross sections [3,5]. The often small one or two-nucleon separation energies led to a successful description in terms of two or three-body structures [6]. This in turn emphasizes the importance of reactions breaking these halo structures into their constituent particles. We shall here concentrate on two-neutron halos where the three-body problem is then inherent. Absolute values for dissociation cross sections of these systems are available in a number of cases [7–13]. They may be divided into processes like one or two neutron knockout arising from Coulomb or nuclear dissociation. Also core destruction processes were studied [14] and the total interaction cross section obtained [3].

Theoretical investigations of two-neutron dissociation cross sections are available on light [15–17] as well as heavy [5,18,19] targets, but core destruction processes are usually not computed at all. Total interaction cross sections for light targets are also calculated for three-body halos [15,20]. However, systematic studies of all these processes within one consistent model are not available. Such results even for relative quantities are rather scarce [17]. Reliable nuclear model estimates of absolute values are in general very difficult. In particular the necessary simultaneous treatment of the Coulomb and nuclear interactions has not been available for these three-body halo reactions.

The lack of systematic experimental and theoretical information about the many different absolute dissociation cross sections is perhaps surprising, but in any case unfortunate, since characteristic features of the reaction mechanism probably can be uncovered by such investigations. The purpose of this letter is then to study all possible three-body dissociation cross sections of two-neutron halo nuclei as functions of target and beam energy. The predictions employ a consistent three-body model and an appropriate reaction framework including simultaneous treatment of Coulomb and nuclear interactions.

*Theoretical formulation.* We shall here only give a brief sketch of the model leaving the details for a more comprehensive publication. We want to describe collisions of a target and a weakly bound two-neutron halo nucleus and classify the cross sections according to the particles left in the final state, i.e.  $\sigma_{nnc}$ ,  $\sigma_{nc}$ ,  $\sigma_{nn}$ ,  $\sigma_c$ ,  $\sigma_n$ ,  $\sigma_0$ , where  $c$  and  $n$  denote core and neutron, respectively and 0 indicates that all particles are absorbed.

The collisions can approximately be described by three independent collisions of one particle (participant) at a time and undisturbed motion of the remaining two projectile particles (spectators) [17]. The interconnected main assumptions are that the halo is weakly bound, spatially extended and the intrinsic halo motion is slow compared to the relative projectile-target motion.

In this simple picture the spectators are always found in the final state while the participant can be either absorbed or scattered by the target. However the finite extension of the projectile constituents and the target is destroying this simple picture, since simultaneous collisions of more than one projectile constituent with the target are possible.

The simplest description of the constituent-target interaction can be made through the black sphere model. This model assumes that a particle is absorbed when passing inside a cylinder with the axis along the beam direction and left untouched otherwise. The radius of this cylinder is approximately equal to the sum of the target and constituent radii. Different contributions to the cross section have to be considered, *i*) three contributions where only one of the constituents is inside the cylinder (one participant and two spectators). In this case the interaction between the participant and the target is described by the phenomenological optical model, and only the part of the three-body wave function where the two spectators are far enough from the participant is included [17]. *ii*) Three contributions where two constituents are inside the cylinders. In this case, the interaction between one of them (participant) and the target is described by the optical model, while for the second constituent-target

interaction we use the black sphere model. To implement this we include only the part of the wave function where the second constituent is close to the participant and the third one is far enough away. *iii*) One contribution where the three constituents are inside the cylinders. Again the interaction of one of the constituents (participant) with the target is described by the optical model, and for the other two we use the black sphere model (only the part of the wave function where the three particles are close enough is included). It is then clear that the distances between the participant and the other two constituents appear as the decisive quantities determining if more than one particle interacts simultaneously with the target. These distances depend on the sizes of the constituents and the target and they are determined as in [17].

In the contributions to *ii*) and *iii*) the participant has to be chosen, and the participant-target interaction is described by the optical model. Since the core-target interaction contains nuclear and Coulomb forces a more careful treatment is required in this case. Therefore the contributions arising from simultaneous interactions of the core and one or two neutrons with the target are computed with the core as participant and the core-target interaction described by the optical model.

The division into different contributions implicitly assumes that for large impact parameters the constituent and the target are not interacting. Obviously this is not true for the long-range Coulomb interaction. To solve this problem, when the core is the participant, we include into the contributions *i*), *ii*) and *iii*) only the large momentum transfer part (low impact parameter) of the Coulomb interaction. The low momentum transfer contribution (large impact parameter) is considered as a process where the core is elastically scattered by the target (via Coulomb interaction) and the two neutrons survive untouched in the final state. The value of the momentum transfer dividing into low and large impact parameters is given by [21]  $q_g = Z_0 Z_i e^2 (\gamma + 1) / (c\gamma\beta(R_0 + R_i + \pi a/2))$ . Here  $R_0$  and  $R_i$  are charge root mean square radii of the target and the core participant ( ${}^9\text{Li}$  or  ${}^4\text{He}$ ) and  $a$  is half the distance of closest core-target approach,  $eZ_0$  and  $eZ_i$  are the charges of the target and participant,  $\beta = v/c$  and  $\gamma = 1/\sqrt{1-\beta^2}$ . The momentum cutoff parameter  $q_g$  separates between impact parameters smaller and larger than the sum of participant and target radii. In the present context this means distinction between absorption (destruction) and survival of the participant.

The differential cross sections arising from participant  $i$  with mass  $m_i$  and charge  $eZ_i$  has contributions from elastic scattering  $\sigma_{el}^{(oi)}$  (diffraction) and absorption  $\sigma_{abs}^{(oi)}$  (stripping) on the target. For a spinless target of mass  $m_0$  and charge  $eZ_0$  we get in the rest system of the halo

$$\frac{d^6 \sigma_{abs}^{(i)}(\mathbf{p}'_{0i,jk}, \mathbf{p}'_{jk})}{d\mathbf{p}'_{0i,jk} d\mathbf{p}'_{jk}} = \sigma_{abs}^{(oi)}(p_{0i}) |M_s(\mathbf{p}_{i,jk}, \mathbf{p}'_{jk})|^2, \quad (1)$$

where  $M_s$  is the normalized overlap matrix element be-

tween initial and final state spectator wave functions,  $\mathbf{p}'_{0i,jk}$  is the relative momentum in the final state between center of mass of target-participant and the spectators  $j$  and  $k$ , while  $\mathbf{p}'_{jk}$ ,  $\mathbf{p}_{0i}$  and  $\mathbf{p}_{i,jk}$  correspondingly are relative momenta between particles  $j$  and  $k$ , 0 and  $i$ ,  $i$  and center of mass of  $j$  and  $k$ . Primes denote final states. Momentum conservation in the rest frame of the projectile gives the relation  $\mathbf{p}'_{0i,jk} = \mathbf{p}_{i,jk} + \mathbf{p}_0(m_j + m_k)/(m_0 + m_i + m_j + m_k)$ , where  $\mathbf{p}_0$  is the momentum of the target.

The differential elastic cross section is

$$\frac{d^9 \sigma_{el}^{(i)}(\mathbf{p}'_{0i,jk}, \mathbf{p}'_{jk}, \mathbf{p}'_{0i})}{d\mathbf{p}'_{0i,jk} d\mathbf{p}'_{jk} d\mathbf{p}'_{0i}} = \frac{d^3 \sigma_{el}^{(oi)}(\mathbf{p}_{0i} \rightarrow \mathbf{p}'_{0i})}{d\mathbf{p}'_{0i}} \times (1 - |\langle \Psi | \exp(i\delta\mathbf{q} \cdot \mathbf{r}_{i,jk}) | \Psi \rangle|^2) |M_s(\mathbf{p}_{i,jk}, \mathbf{p}'_{jk})|^2, \quad (2)$$

where  $\Psi$  is the initial three-body halo state. We have now a 9-dimensional differential cross section, since the participant explicitly is included in the final state. The momentum  $\delta\mathbf{q} = (\mathbf{p}'_{i,jk} - \mathbf{p}_{i,jk})(m_j + m_k)/(m_i + m_j + m_k)$  is the transfer into the participant-spectators relative motion described by the coordinate  $\mathbf{r}_{i,jk}$ . The second factor in eq.(2) then expresses the probability for the halo *not* ending up in its ground state. In this way we remove elastic scattering of the halo as a whole.

When the participant is charged the Coulomb interaction produces a logarithmic divergence in the total cross section Eq.(2). The corresponding adiabatic motion related to virtual excitations at large impact parameters should be removed from the dissociation cross sections [21]. We therefore exclude contributions from momentum transfer smaller than the adiabatic cutoff  $q_a = \hbar Z_0 Z_i e^2 / (\pi \hbar c) B_{ps} / (\hbar c) (\gamma + 1) \gamma^{-2} \beta^{-2}$ , where  $B_{ps}$  is the binding energy between participant and the system consisting of the spectators, i.e.,  $B_{ps} = B - B_{2s}$ , where  $B$  is the three-body binding energy and  $B_{2s}$  is the two-body binding energy of the two spectators. Note that in a Borromean nucleus  $B_{2s}$  is negative.

The energy transferred from target to participant,  $\delta E \equiv \sqrt{\mathbf{p}_0^2 + m_0^2} - \sqrt{\mathbf{p}'_0{}^2 + m_0^2}$ , must be larger than  $B$ . When  $\mathbf{p}_0$  and  $\mathbf{q} \equiv \mathbf{p}_0 - \mathbf{p}'_0$  are parallel  $\delta E$  is maximized. For this geometry we find for small  $B$  compared to the target rest mass that  $\delta E = B$  implies that  $q_c \equiv q_{LC} \approx B\sqrt{1 + m_0^2 c^2 / p_0^2}$  which reduces to  $B/v$  in the non-relativistic limit. Thus  $q$  must be larger than  $q_L$  to produce dissociation, but on the other hand dissociation is not the necessary outcome for all  $q > q_L$ . In the computations we exclude contributions from momentum transfer  $q$  smaller than the largest of  $q_L$  and  $q_a$ .

*Cross sections.* The model is now completely defined with both Coulomb and nuclear interactions included for weakly bound three-body halo reactions. We shall study breakup reactions of  ${}^6\text{He}$  and  ${}^{11}\text{Li}$  on C, Cu, and Pb targets. The parameters corresponding to the  ${}^6\text{He}$  and  ${}^{11}\text{Li}$  wave functions are obtained from [17,19]. The optical model parameters are from [22] for neutrons, from [23] for  $\alpha$ -particles and for  ${}^9\text{Li}$  also from [23] but using range and

diffuseness parameters from [24]. We furthermore drastically reduce the energy dependence of the real part of the potential in [23], i.e.  $a_2 = -0.014$ , to allow for the required huge beam energy variation. The measured core-target interaction cross sections are reproduced within error bars [9]. The binding energy  $B_{ps}$  between the  $^9\text{Li}$  and  $^4\text{He}$  cores and the two neutrons must be introduced for the adiabatic cutoff. We use the scaling relation in [25] to obtain  $B_{ps}/B \approx 3$  for  $^6\text{He}$  and 1.4 for  $^{11}\text{Li}$ .

The corresponding contributions to the dissociation cross sections are obtained as indicated in *i*), *ii*) and *iii*) by integration of Eqs.(1) and (2). The cross sections are then classified according to the particles left in the final state, i.e.  $\sigma_{nnc}$ ,  $\sigma_{nc}$ ,  $\sigma_{nn}$ ,  $\sigma_c$ ,  $\sigma_n$ , and  $\sigma_0$ . Specific interesting cross section combinations are those of two-neutron removal  $\sigma_{-2n} \equiv \sigma_{nnc} + \sigma_{nc} + \sigma_c$ , core destruction  $\sigma_{-c} \equiv \sigma_{nn} + \sigma_n + \sigma_0$  and the sum of these, the total interaction cross section  $\sigma_I \equiv \sigma_{-2n} + \sigma_{-c}$ .

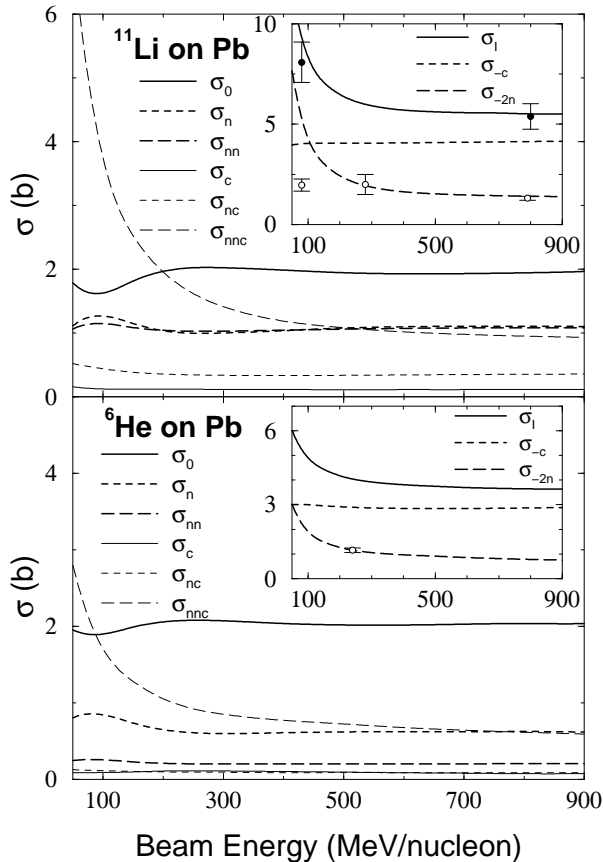


FIG. 1. Dissociation cross sections as function of beam energy for fragmentation of  $^{11}\text{Li}$  (upper part) and  $^6\text{He}$  (lower part) on a Pb-target. The labels indicate the halo particles in the final state. The inset shows  $\sigma_{-2n} = \sigma_c + \sigma_{nc} + \sigma_{nnc}$ ,  $\sigma_{-c} = \sigma_0 + \sigma_n + \sigma_{nn}$ ,  $\sigma_I = \sigma_{-2n} + \sigma_{-c}$ . The experimental data are from [8,9,11,13].

In fig. 1 we show the results for a lead target and  $^{11}\text{Li}$  (upper part) and  $^6\text{He}$  (lower part) projectiles. At low

beam energies  $\sigma_{nnc}$  is the dominant cross section, especially in the  $^{11}\text{Li}$  case. This is due to the large Coulomb interaction, that highly increases the large impact parameter contribution (where the two neutrons both survive

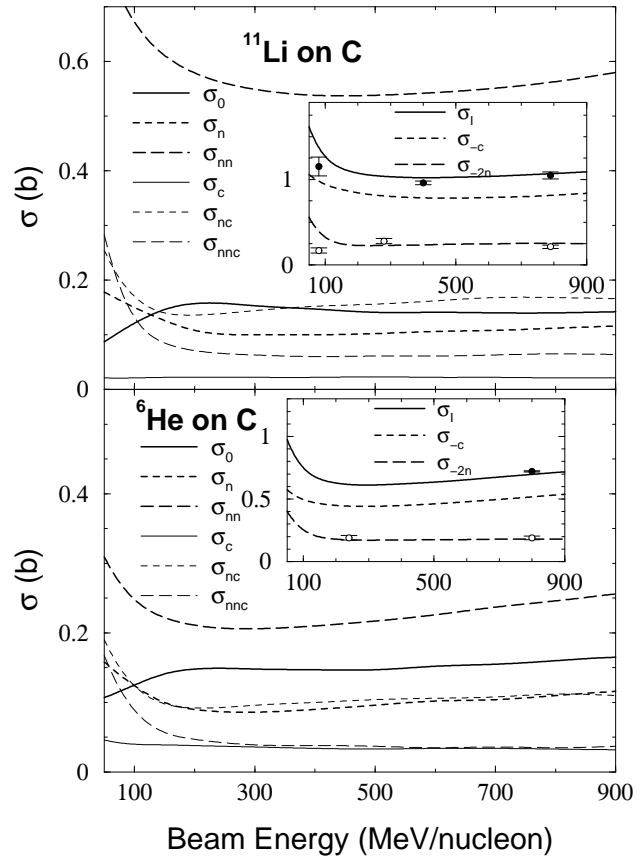


FIG. 2. The same as Fig.1 for a C-target. The experimental data are from [7,9,11,13,15].

in the final state). The  $\sigma_{nnc}$  cross section rapidly decreases with the beam energy, and for energies larger than 200 MeV/nucleon in the  $^{11}\text{Li}$  case and 100 MeV/nucleon in the  $^6\text{He}$  case  $\sigma_0$  dominates (no particles in the final state). The reason for this is the large radius of the Pb-target, resulting in a very high probability for finding all the three projectile constituents inside the absorption cylinders. This probability is higher for  $^6\text{He}$  projectile than for  $^{11}\text{Li}$ , because from the three-body wave function we get  $\langle r_{cn}^2 \rangle^{1/2} = 4.2$  fm in the first case and 5.9 fm in the second ( $r_{cn}$  = neutron-core distance). As a consequence, when the core is the participant, 85% of the  $^6\text{He}$  wave function corresponds to all three constituents inside the cylinders and only 65% for the  $^{11}\text{Li}$  projectile. This is reflected in the figure by the fact that  $\sigma_0$  takes very similar values in both cases, while as a general rule the cross sections for  $^{11}\text{Li}$  should be larger than the ones for  $^6\text{He}$ . The core destruction cross section  $\sigma_{-c} = \sigma_0 + \sigma_n + \sigma_{nn}$  is shown in the insets by the short-dashed line. Its behavior is determined by the core-Pb absorption cross section,

and changes very little with the beam energy. The two-neutron removal cross section  $\sigma_{-2n} = \sigma_{nnc} + \sigma_{nc} + \sigma_c$  is shown as the long-dashed lines in the insets, and it is given by all the processes where the core survives and contains therefore the contribution from the Coulomb interaction. Therefore this cross section decreases with beam energy. Finally the solid lines in the insets show the

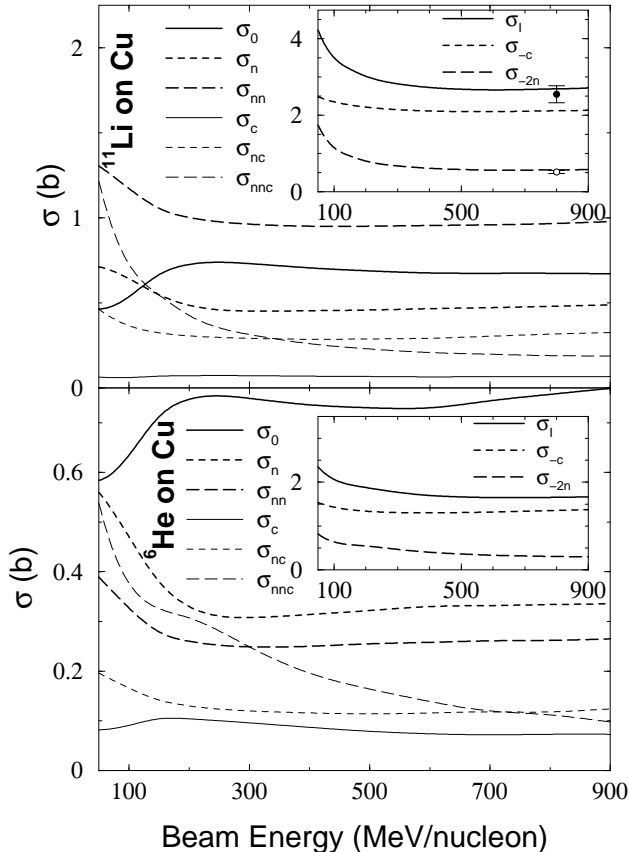


FIG. 3. The same as Fig.1 for a Cu-target. The experimental data are from [8].

interaction cross section  $\sigma_I = \sigma_{-2n} + \sigma_{-c}$ . The agreement with the experimental data is remarkably good.

In fig. 2 we show the results for a light target (carbon) where the cross sections are up to a factor of 10 smaller than for a lead target. The main difference is that the effect produced by the Coulomb interaction is now small, and for example  $\sigma_{-2n}$  is determined by Coulomb for Pb and by nuclear interactions for C targets. The dominating cross section is now  $\sigma_{nn}$  for C instead of  $\sigma_{nnc}$  or  $\sigma_0$  for Pb targets. The reason is that the small radius of the target diminishes the probability of simultaneous interaction of more than one constituent with the target, and absorption of the core together with two truly undisturbed spectator neutrons becomes the most likely process. The variation with beam energy is in general rather similar to that of Pb, in particular revealed by  $\sigma_{-c}$ ,  $\sigma_{-2n}$  and  $\sigma_I$  shown in the insets. Also in this case we obtain good agreement with the experimental data.

In fig. 3 we show the results for a copper target, i.e. an intermediate mass with comparable Coulomb and nuclear contributions. The cross sections are between those obtained for carbon and lead with similar energy dependences. However,  $^{11}\text{Li}$  has a larger radius than  $^6\text{He}$ . Thus the dominating cross section for  $^{11}\text{Li}$  is  $\sigma_{nn}$  as for carbon, while  $\sigma_0$  dominates for  $^6\text{He}$  as for a lead target.

Only a few of the computed cross sections are experimentally available. In [13] experimental data for  $\sigma_{nnc}$ ,  $\sigma_{nc}$  and  $\sigma_c$  are given for  $^6\text{He}$  on C and Pb at 240 MeV/nucleon. In [11] the experimental data for the same cross sections are given for  $^{11}\text{Li}$  fragmentation on C and Pb at 280 MeV/nucleon. Also in [16]  $\sigma_{nnc}$ ,  $\sigma_{nc}$  and  $\sigma_c$  are calculated for  $^{11}\text{Li}$  and  $^6\text{He}$  on C by use of the eikonal theory. In table I we compare the results of our calculation with the ones given in [16] and the experimental data in [11,13]. For carbon target the agreement with the experimental data and previous calculations is good. The only significant deviation is in  $\sigma_{nc}$  for the case of lead target, where our calculation gives a cross section at least a factor of two smaller than the experimental value.

Target	$^6\text{He}$ (240 MeV/nucleon)			$^{11}\text{Li}$ (280 MeV/nucleon)			
		$\sigma_{nnc}$	$\sigma_{nc}$	$\sigma_c$	$\sigma_{nnc}$	$\sigma_{nc}$	$\sigma_c$
C	Exp. [11,13]	$30 \pm 5$	$127 \pm 14$	$33 \pm 23$	$60 \pm 20$	$170 \pm 20$	$50 \pm 10$
	This work	43	93	37	64	142	22
	Ref. [16]	32	136	17	6-10	121-162	27-40
Pb	Exp. [11,13]	$650 \pm 110$	$320 \pm 90$	$180 \pm 100$	$1000 \pm 350$	$1000 \pm 350$	$\leq 70$
	This work	940	96	113	1476	338	116

TABLE I. Computed values of  $\sigma_{nnc}$ ,  $\sigma_{nc}$  and  $\sigma_c$  for  $^6\text{He}$  on C and Pb at 240 MeV/nucleon and for  $^{11}\text{Li}$  on C and Pb at 280 MeV/nucleon. For comparison we give the results reported in [16]. Experimental data from [11,13].

The core destruction processes entering in  $\sigma_{-c}$  all must take place at small impact parameters. The Coulomb contributions are therefore relatively unimpor-

tant in contrast to the large impact parameter processes where purely Coulomb dissociation reactions take place. Coulomb dissociation cross sections have been previously

estimated in models where the three-body system is treated as an effective two-body (dineutron plus core). For  $^{11}\text{Li}$  on lead at 800 MeV/nucleon we get 765 mb, while in [25] they obtain 960 mb, and in [26] they report values ranging from 610 to 660 mb. For  $^{11}\text{Li}$  on Cu at 800 MeV/nucleon we obtain a Coulomb dissociation cross section of 81 mb, while in [26] they give values from 86 to 92 mb. Calculations where the final continuum three-body wave function is considered are also available [19]. For  $^{11}\text{Li}$  on Pb at 180, 280, and 800 MeV/nucleon they get 2128 mb, 1429 mb and 971 mb, respectively, while our calculations for the same energies give 2050 mb, 1401 mb and 765 mb. These rather few previous computations where a comparison is possible are in general in rough agreement with our systematic results.

*Conclusion.* We have computed all possible three-body dissociation cross sections of two-neutron halos as function of beam energy and target. Coulomb and nuclear interactions are treated within the same framework. The available experimental information, mostly about total interaction and two-neutron separation cross sections, compares rather well with the calculated results, especially at high energies. At low energies the three-body continuum final state might turn out to be more appropriate. The further division into a specific number of particles in the final states carries detailed information about the reaction mechanism. We predict the absolute sizes of all these cross sections to encourage new measurements.

*Acknowledgement.* We thank K. Riisager for continuous discussions and suggestions.

---

[1] K. Riisager, Rev. Mod. Phys. **66** (1994) 1105.

- [2] P.G. Hansen, A.S. Jensen and B. Jonson, Ann. Rev. Nucl. Part. Sci. **45** (1995) 591.
- [3] I. Tanihata, J. Phys. **G22** (1996) 157.
- [4] B. Jonson and K. Riisager, Phil. Trans. R. Soc. Lond. **A356** (1998) 2063.
- [5] C.A. Bertulani, L.F. Canto and M.S. Hussein, Phys. Rep. **226** (1993) 281.
- [6] M.V. Zhukov, B.V. Danilin, D.V. Fedorov, J.M. Bang, I.J. Thompson and J.S. Vaagen, Phys. Rep. **231** (1993) 151.
- [7] I. Tanihata et al., Nucl. Phys. **A488** (1988) 113c.
- [8] T. Kobayashi et al., Phys. Lett. **B232** (1989) 51.
- [9] B. Blank *et al.* Nucl. Phys. **A555** (1993) 408.
- [10] F. Humbert *et al.*, Phys. Lett. **B347** (1995) 198.
- [11] M. Zinser et al., Nucl. Phys. **A619** (1997) 151.
- [12] D. Aleksandrov et al., Nucl. Phys. **A633** (1998) 234.
- [13] T. Aumann et al., Phys. Rev. **C59** (1999) 1252.
- [14] T. Nilsson *et al.*, Europhys. Lett. **30** (1995) 19.
- [15] Y. Suzuki, T. Kido, Y. Ogawa, K. Yabana and D. Baye, Nucl. Phys. **A567** (1994) 957.
- [16] G.F. Bertsch, K. Hencken and H. Esbensen, Phys. Rev. **C57** (1998) 1366.
- [17] E. Garrido, D.V. Fedorov and A.S. Jensen, Phys. Rev. **C59** (1999) 1272.
- [18] Y. Ogawa, K. Yabana and Y. Suzuki, Nucl. Phys. **A543** (1992) 722.
- [19] A. Cobis, D.V. Fedorov and A.S. Jensen, Phys. Rev. **C58** (1998) 1403.
- [20] J.S. Al-Khalili and J.A. Tostevin Phys. Rev. Lett. **76** (1996) 3903.
- [21] C.A. Bertulani and G. Baur, Phys. Rep. **163** (1988) 299.
- [22] E.D. Cooper, S. Hama, B.C. Clark and R.L. Mercer, Phys. Rev. **C47** (1993) 297.
- [23] M. Nolte, H. Machner and J. Bojowald, Phys. Rev. **C36** (1987) 1312.
- [24] M. Zahar et al., Phys. Rev. **C54** (1996) 1262.
- [25] L. Johannsen, A.S. Jensen and P.G. Hansen, Phys. Lett. **B244** (1990) 357.
- [26] Y. Suzuki and Y. Tosaka, Nucl. Phys. **A517** (1990) 599.